Experimental Study on the reasonable inbuilt-ring Depth of soil one-dimensional Infiltration Experiment in Field*

Guisheng Fan[1], Yonghong Han[1], Min Song[1]

[1]College of Water Resources Science and Engineering of Taiyuan University of technology
Taiyuan shangxi province, China 030024
Fanguis5507@263.net

Abstract: Based on the field double-ring infiltration experiment under the condition of the same soil and with the different inbuilt-ring depths, the changes of soil cumulative infiltration and infiltration rate with inbuilt-ring depths were analyzed and a reasonable inbuilt-ring depth of the filtration test in field was confirmed. The results indicate that the measured precision of soil infiltration parameters is influenced by the inbuilt-ring depths. Namely, within a certain inbuilt-ring depth range, infiltration rate shows a trend of decreasing with the increasing of inbuilt-ring depth. nevertheless, when the inbuilt-ring depth reaches 19cm to 22cm the Infiltration rate curves are basically coincident. Therefore, the reasonable inbuilt-ring depth of the infiltration experiment in field should be between 19cm and 22cm. Through comprehensive consideration of the measurement accuracy, test instrument cost and test labor intensity, the reasonable inbuilt-ring depth of infiltration experiment in field can be targeted for 19cm if plough depth is less than 20cm; otherwise, the inbuilt-ring depth can be 20cm to 22cm.

Key words: Double-Ring Infiltrometer, Inbuilt-Ring Depth, Infiltration Rate; Lateral Infiltration, Soil Moisture Infiltration

1. Introduction

Double-ring infiltrometer is the most commonly used to measure the infiltration parameters of field soils. Its working principle is that the condition of one-dimensional vertical downward motion of soil moisture is formed in the inner rings with the help of the homocentric outer rings embedded in certain depth below the surface, and through measuring the infiltrating water amount in the inner rings the infiltration process and parameters of soils are obtained. The buried depth of homocentric inner and outer rings below the surface is defined as inbuilt-ring depth. At present, the international standards about double-ring infiltration apparatus is as follows, inner ring is 20cm high and inner diameter is 26.2cm; outer ring is 20cm high and inner diameter is 60cm; both the inbuilt-ring depth are 10cm. several decade field infiltration test datum obtained by writer with the standard double-ring infiltration apparatus showed that the height of the standard ring is not enough for obtaining the accurate test datum, the inbuilt-ring depth is lacking and the soil infiltration capacity measured is deflective. Therefore, writer had processed a set of d double-ring infiltration apparatus with different ring heights and had performed a series of soil infiltration experiment with different inbuilt-ring depths in the same soil conditions, in order to attempt to explore the reasonable inbuilt-ring depth of double-ring infiltration experiment under the agricultural soil condition. Based on field experimental datum of soil infiltration, the change of soil accumulation infiltration and infiltration rate along with inbuilt-ring depth and the reasonable inbuilt-ring depth was measured. The results provided will be of important values for enhancing the measurement precision of field soil infiltration parameters.

2. Experiment condition

2.1 Soil condition

The tests measuring the influence of inbuilt-ring depth to soil infiltration ability was conducted in Shanxi Province center irrigation experimental station. The station is located in the middle reach of Taiyuan basin where the terrain is flat. The quality of soil material is mainly constituted of the River alluvial and proluvial deposit, and the soil type is moisture soil. The burial depth of Ground water table is between 1.5 and 3.5 meters. The soil plough layer depth is between 18cm and 22cm. The dry density of the surface soils is 1.05g/cm^3,the volumetric water content is 15.9%; in the 10～20cm soil layer, the soil dry density is 1.346g/cm^{3}and the soil volumetric water content is 21.6% ; in the plough bottom layer, the soil dry density is 1.408g/cm^3, and the volumetric water content is 27.1%; the soil dry density at underside of the plough bottom layer is 1.358g/cm^3. the texture of 0-20cm surface soil is loam, clay content (grain size < 0.002mm) is 22.3%, silt content (0.002mm <grain size < 0.05mm) is 47.5%,sand content (grain size > 0.05mm) is 30.2% ; the texture of 20-40cm soil layer is clay loam, clay particle content is 38.2%, silt content is 54.1%,and sand content is7.7% ; the texture of 40-60cm soil layer is sandy loam, clay content is 18.1%, silt content is 45.7%,and sand content is 36.2%.

2.2 Experiment equipment

Three pieces of equipment were used in the tests. One is the international standard double-ring infiltration experiment which was manufactured by Northwest water resources research institute, the height of inside and outside rings is separately 20cm and 26cm, the inbuilt-ring depth into soils is 10cm.It is made of stainless steel. There are two stainless steel slices fixed symmetrically on both sides of the inside ring to control inbuilt-ring depth. Other two infiltration equipments is self-regulating, the inside ring diameter is 26cm,outside ring diameter is 64.4cm,the maximal inbuilt-ring depth of inside and outside rings can respectively reach 20cm and 25cm.

2.3 Experiment program

In the selected test field, a set of soil infiltration tests were proceeded under the same soil condition, the inbuilt-ring depth is singly 10cm、13cm、16cm、19cm and 22cm.The aim of the experiment was to reveal influence of inbuilt-ring depth to soil infiltration rate, and to ascertain the reasonable inbuilt-ring depth of field infiltration experiment. To ensure the consistency of the tested soil conditions, five infiltration tests with different inbuilt-ring depth were arranged within small plot with 3m×3m scale.

The tested time was identified as 90min (At this time, soil moisture infiltration rate of all tests reach relatively stable rate), in the ahead two minutes after infiltration begin, the long of each observed time interval was 30 seconds; within 2-15 minutes was 60-180 seconds; within 15-60 minutes was 300 seconds; after 60 minutes was 600 seconds.

3 Experimental results and analysis

3.1 Influence of inbuilt-ring depth on infiltration processes

Fig.1 shows soil cumulative infiltration amount and infiltration rate curves with 10cm and 22cm inbuilt-ring depths in the same soil condition where moisture content, soil structure, content of organic matter, salinity content were the same .From fig.1 it can be aware that the influence of inbuilt-ring depth on soil infiltration processes and capacity was obviously.

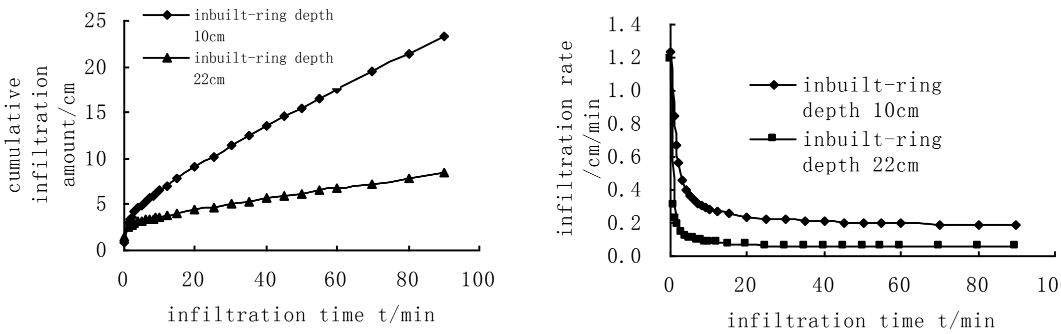

1-a Hydrograph of soil cumulative infiltration amount along with time

1-b Hydrograph of soil infiltration rate along with time

Fig.1 Soil accumulative infiltration amount and infiltration rate curves with different inbuilt-ring depths

In Fig.1-a, it shows that the soil cumulative infiltration curve with 10cm inbuilt-ring depth is all along above the cumulative infiltration curve with 22cm inbuilt-ring depth, the cumulative infiltration amount within 90 minutes of the former is 23.3cm which is more twice than 8.381cm of the latter. Thus it can be seen that infiltration amount of the former was much larger than the latter. In Fig.1-b, the soil infiltration rate with 10cm inbuilt-ring depth is bigger than with 22cm inbuilt-ring depth, the relative steady infiltration rate of the former is 0.1889cm/min which is three times more than 0.0535cm/min with 22cm inbuilt-ring depth. By the above contrast of the infiltration rate and cumulative infiltration amount, it is showed that the measured infiltration capacity with small inbuilt-ring depth is greater than with big inbuilt-ring depth. therefore, inbuilt-ring depth had an distinct affect on the measured value of soil infiltration capacity. The deviation value should be occurred by the different lateral infiltration amount round the infiltration rings with different inbuilt-ring depths.

Fig.2 indicates the lateral infiltration processes generating in double-ring infiltration test.

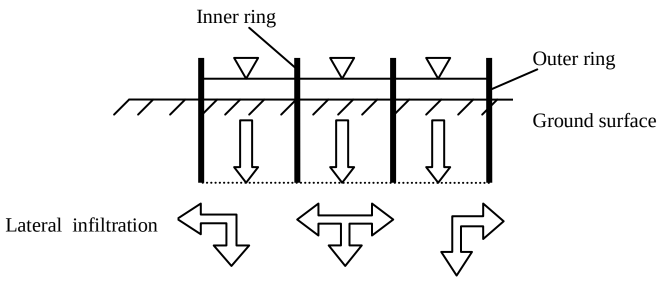

Fig.2 Sketch map of lateral infiltration generating process in union thimbles infiltration experiment

Specific process of the lateral infiltration is as follows. Before moisture infiltration front arrives below interface of ring (such as 10cm), due to the hinder of inner and outer impervious ring wall, moisture infiltration belongs to the strict one-dimensional vertical infiltration, where no lateral infiltration takes place. After moisture infiltration front gets to 10cm depth, lateral infiltration begins to occur firstly in outer ring. The dynamical mechanism is that horizontal water potential gradient which is caused by inner and outer moisture content difference of outer ring boundary wall drove soil moisture migrate from outer ring inside to outer ring outside, namely, the moisture content in outer ring inside boundary overtops the moisture content in outer ring outside boundary, soil matrix potential of outer ring boundary inside is higher than outside.

Along with the happening of lateral infiltration on outer ring boundary, the advancing speed of infiltration stream vertical front in outer ring slows down, while the advancing of infiltration stream vertical front in inner ring keeps normal, which leads to the results that on the same horizontal surface, the soil moisture content in inner ring exceeds that in outer ring, a horizontal matrix potential gap between the inner ring and the outer ring is formed, and then infiltration stream moves from the inner ring to the outer ring. Namely, one-dimensional vertical infiltration condition is broken and lateral moving of infiltration stream in the inner ring occurs.

By above analysis, following conclusion is easily gained. Theoretically, no matter how much inbuilt-ring depth is, as long as infiltration time is enough long, lateral infiltration will emerge in both inner and outer rings. Here the key problem is explaining why the lateral infiltration of shallow inbuilt-ring depth is bigger than deep inbuilt-ring depth. Hereon and Green-Ampt infiltration pattern is introduced to explain the phenomenon. Model sketch map is showed in Fig.3.In Fig.3, Zf_{22} and Zf_{10} respectively are infiltration wetting front position with 22cm and 10cm inbuilt-ring depth, $\triangle x_{22}$ and $\triangle x_{10}$ respectively are sometime lateral infiltration travel length of 22cm and 10cm, i.e. horizontal infiltration distance $\triangle x$ which changes with time.

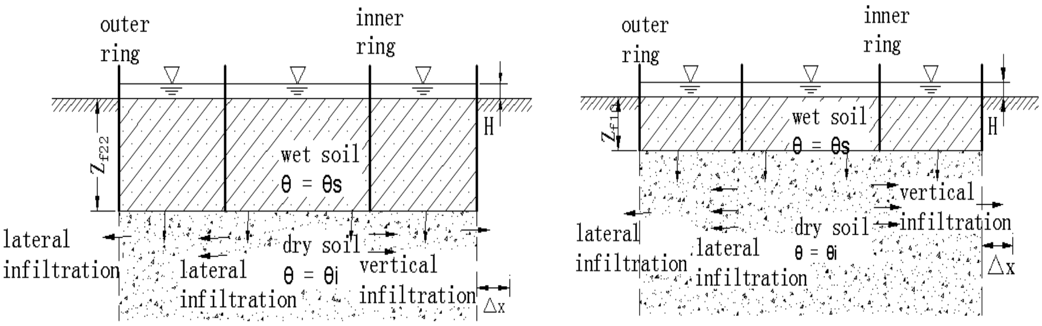

Fig.3 Pattern sketch map with 22cm and 10cm inbuilt-ring depth

Based on the capillary theory, the infiltration problem of initial dry soil with lamina ponding on soil surface was researched with the help of Green-Ampt pattern. The pattern assumes are as follows: a horizontal wetting front exists definitely during soil moisture infiltrating, humid and non- humid region are separated by the horizontal wetting front, soil moisture content distribution is with ladder shape, moisture content in humid region is saturated content θ_s, soil moisture content underneath the wetting front is initial moisture content θ_i. Surface ponding depth is supposed as H and is not mutative along with time, the position of wetting front is $z_f(t)$ and migrated with infiltration time. Soil water suction underneath the wetting front is s_f and is considered as a fixed value. Z coordinate origin zero is set on the surface, was positive downward. The total water potential on the surface is H ,on the wetting front was $-(s_f + z_f(t))$, therefore, water potential gradient is $[-(s_f + z_f(t)) - H]/z_f(t)$ .The flux from surface into soil, that in essence is the infiltration rate $i(t)$ of the surface was gotten by Darcy law.

$$i(t) = K_s \frac{z_f(t) + s_f + H}{z_f(t)} = K_s\left[1 + \frac{s_f + H}{z_f(t)}\right] \tag{1}$$

Formula (1) shows the relation between infiltration rate $i(t)$ and wetting front $z_f(t)$ .Here: K_s is saturated hydraulic conductivity.

Formula (1) is vertical infiltration rate formula. A formula of horizontal infiltration rate $i'(t)$ representing lateral infiltration can be derived from vertical infiltration rate formula. Because the lateral infiltration is horizontal, the gravity potential gradient in horizontal direction is inexistent. Therefore, formula (1) could be turned into as follow:

$$i'(t) = K_s \left[\frac{s_f + H + z_f(t)}{\Delta_x(t)} \right] \tag{2}$$

Next, On the basis of formula (2), it is analyzed why lateral infiltration of shallow inbuilt-ring depth is bigger than deep inbuilt-ring depth (taking 10cm and 22cm for instance).As it is seen from formula (2) that the value of $i'(t)$ is depended on the two items K_s and $\frac{s_f + H + z_f(t)}{\Delta_x(t)}$. The effect of the two items to lateral infiltration rate are separately analyzed as follow.

(1) Soil saturated hydraulic conductivity is related to soil texture and soil volume weight, the value becomes smaller when soil becomes dense and viscous. When inbuilt-ring depth is 10cm, Lateral infiltration occurs at 10cm depth, where the soil layer is located in plough layer, the soil type is loam, the soil volume weight is 1.05g/cm^3, the soil texture was lighter and volume weight was smaller. When inbuilt-ring depth is 22cm, lateral infiltration occurs at 22cm depth, where the soil layer is located in plough pan, the soil type is clay loam, the soil volume weight is 1.408g/cm^3, the soil texture was heavier and volume weight was bigger. Therefore, K_{s22} of the latter is less than K_{s10} of the former.

(2) In the item $\frac{s_f + H + z_f(t)}{\Delta_x(t)}$, surface ponding depth H is definite value, soil water suction s_f in wetting front is related to soil moisture content, the value of s_f becomes smaller along with increasing of moisture content. When inbuilt-ring depth is 10cm, the soil moisture content at 10cm depth where lateral infiltration occurs initially is 15.9%, while the soil moisture content at 22cm depth where lateral infiltration occurs initially is 27.1% .Therefore, s_f of the latter is less than the former, namely, $s_{f22} < s_{f10}$. $z_f(t)$ expresses wetting front position. the value of 22cm and 10cm inbuilt-ring were 0.22 and 0.1.So following formula (3) is got.

$$\frac{s_{f22} + H + 0.22}{\Delta_{x22}(t)} < \frac{s_{f10} + H + 0.1}{\Delta_{x10}(t)} \tag{3}$$

By synthesizing above analyses, it can be achieved that the lateral infiltration rate with 22cm inbuilt-ring depth is smaller than with 10cm, namely, $i'_{22}(t) < i'_{10}(t)$.Meanwhile, because the starting time of lateral infiltrating with 22cm inbuilt-ring depth is posterior to with 10cm, the sustain time for lateral infiltrating is shorter, and the soil area of the lateral infiltrating with 22cm inbuilt-ring depth is smaller than with 10cm. Therefore, the infiltration rate with 22cm inbuilt-ring depth was smaller than with 10cm, and the lateral infiltration rate with shallow inbuilt-ring depth is bigger than with deep inbuilt-ring depth.

3.2 Quantitative influence of Inbuilt-ring depth on infiltration capacity

Fig.4 shows five sets of accumulative infiltration curve and infiltration rate curve under the same soil conditions and with different Inbuilt-ring depths.

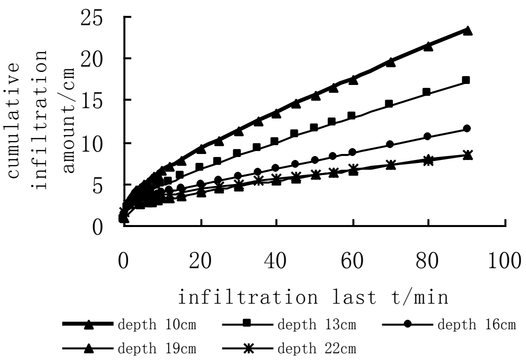

Figure 4-a Changing curves of the cumulative infiltration amount at given time with different depths

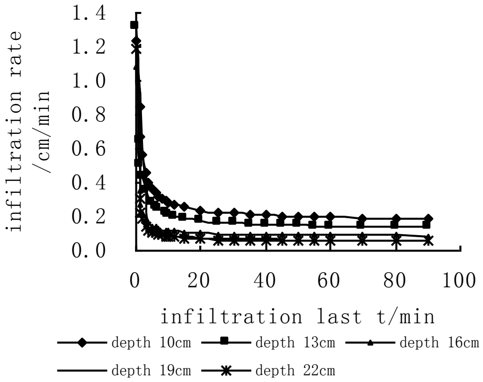

Figure 4-b Changing curves of the infiltration rate at given time with different depths

Fig.4 soil infiltration curves with different Inbuilt-ring depths

From Fig.4, following outcomes can be got.

(1) The Cumulative infiltration curves with shallow inbuilt-ring depths are always above the curves with deep inbuilt-ring depths. In Fig.4, when inbuilt-ring depth increases from 10cm to 22cm, the cumulative infiltration amount at 90 minutes reduces from 23.302 cm to 9.381cm.

(2) From Fig.4-a, it can be seen that when the inbuilt-ring depth increases to over 19cm, cumulative infiltration curves overlaps. Namely, the cumulative infiltration curve with 19cm inbuilt-ring depth overlaps basically with the curve with 22cm inbuilt-ring depth.

(3) Fig.4-b indicated that during the whole process of infiltration, the infiltration rate curves with shallow inbuilt-ring depths are always above the curves with deep depth. When inbuilt-ring depth increases from 10cm to 22cm, the infiltration rate at 90min reduces from 0.1889cm/min to 0.0535cm/min.

(4) When the inbuilt-ring depth increases to over 19cm, the infiltration rate curves overlaps nearly, namely, the infiltration rate curves of 19cm and 22am overlap basically.

The analysis above indicates adequately that inbuilt-ring depth has obvious influence on determining of soil infiltration capacity, along with the increasing of inbuilt-ring depth, measured cumulative infiltration amount and infiltration rate reduces, after the inbuilt-ring depth increases to 19cm the measured values are inclined to stabilizing instead of decreasing, namely, the curves of 19cm and 22cm overlap basically. Consequently After the inbuilt-ring depth achieves over 19cm infiltration processes is not influenced by inbuilt-ring depth.

Fig.5 and Fig.6 present respectively the changing curve of the cumulative infiltration amount at 90 minutes with inbuilt-ring depths and the changing curve of the steady infiltration rate at 90 minutes with inbuilt-ring depths.

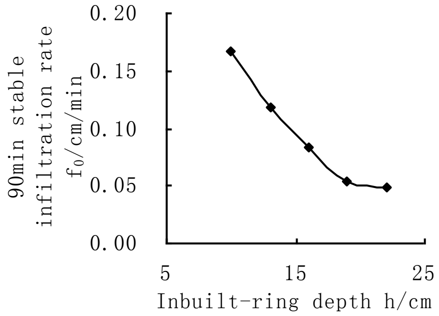

Fig.5 Changing curve of the cumulative infiltration amount at 90 minutes with inbuilt-ring depths

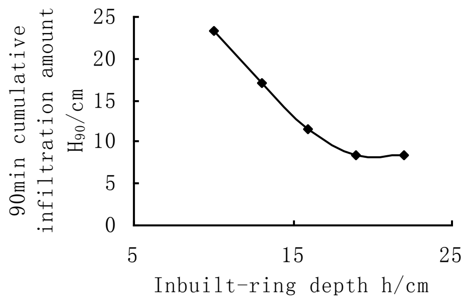

Fig.6 Changing curve of the infiltration rate at 90 minutes with inbuilt-ring depths

(1) In Fig.5, the changing curve of the cumulative infiltration amount at 90 minutes presents a reductive trend with the increase of inbuilt-ring depth and tends to stable after inbuilt-ring depth increases to more than 19cm.As showed in Fig.5, H_{90} of 19cm is 8.506cm and H_{90} of 22cm is 8.381cm.

(2) In Fig.6, the steady infiltration rate at 90 minutes presented a decreasing trend with the increasing of inbuilt-ring depth, last, the curve tended to horizontal. As Fig.6 showed, f_0 of 19cm is 0.0538cm/min and f_0 of 22cmis 0.0489 cm/min.

According to Fig.5 and Fig.6, following outcome can be got. After inbuilt-ring depth reaches more than 19cm, the cumulative infiltration amount and infiltration rate at 90min all tends to basically stable, which shows that when the inbuilt-ring depth reaches more than 19cm, soil moisture infiltration has reached a relatively stable level.

3.3 Reasonable inbuilt-ring depth

Factors which should be considered in determining reasonable inbuilt-ring depth should be as follows:

(1) Certain measurement precision should be guaranteed. The measured value should be close to the true value. Upper segment analysis shows that when the inbuilt-ring depth into soil were 19～22cm ,the measured infiltration rate already have tended to steady, therefore, the measured value with 22cm inbuilt-ring depth could be as approximation to true value.

(2) Production cost of measuring apparatus should be considered. If inbuilt-ring depth into soil were too shallow, the production cost of measuring apparatus could be reduced, but the required measuring precision could not be achieved; if depths were too deep, though measuring precision could be achieved, production cost of measuring apparatus would increase greatly.

(3) Difficulty and Labor intensity of driving rings into soil should be considered. If the

inbuilt-ring depth was deep, thickness of ring walls should be increased, so the difficulty and labor intensity of driving rings into soil increased.

To determine reasonable inbuilt-ring depth the above three factors must be synthetically considered.

Fig.7 shows cumulative infiltration amount curve at each given time with different inbuilt-ring depths. In Fig.5, H_{10} signified cumulative infiltration amount at 10min after tests begin, and so on. From Fig.5,it could be discovered that at every given moment, the cumulative infiltration amount presents the same variation trend. Namely Along with increasing of the inbuilt-ring depth, the every given moment, the cumulative infiltration amount decreases, and when depth reach 19cm～22cm the curves became parallel to the horizontal coordinates.

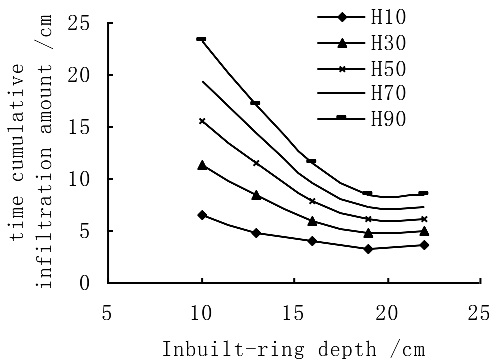

Fig.7 Changing curves of the cumulative infiltration amount at given time with different depths

The measured Value with 22cm inbuilt-ring depth could be considered as standard in order to calculate other depths corresponding relative errors. Table 1 presents the relative error with different inbuilt-ring depth corresponding each given time cumulative infiltration relative to 22cm inbuilt-ring depth. From Table 1, it can be discovered that the relative error of cumulative infiltration amount reduces along with the increase of inbuilt-ring depth; for the same inbuilt-ring depth, the relative error of cumulative infiltration amount reduces along with increase of infiltration time. When the depth achieved above 19cm and infiltration time reached more than 60min,the relative error of cumulative infiltration amount is less than 1.49%.Above analysis makes clear that sideward infiltration aroused by lacking depth has reached negligible level when inbuilt-ring depth reached more than 19cm.Therefore,19～22cm could be defined as reasonable inbuilt-ring depth from the requirements of test precision.

Through analysis above, measurement accuracy would also improve slightly through further enlarged depths, but would increase apparatus production cost, difficulty of inbuilt-ring and labor intensity during the experiments greatly. The following suggestions were putted forward combining years of field infiltration experience of author: if the buried plough bottom was less than 20cm,the inbuilt-ring depth could be 19cm;if the buried plough bottom was more than

20cm,the inbuilt-ring depth could be 20～22cm.

Tab 1 Relative error of the cumulative infiltration amount at given time under different depths relative to 22cm depth

Inbuilt-ring depth (cm)	Relative error（%）								
	the cumulative infiltration amount at given time								
	H_{10}	H_{20}	H_{30}	H_{40}	H_{50}	H_{60}	H_{70}	H_{80}	H_{90}
10	78.61	107.53	126.37	140.21	150.99	159.62	166.81	172.85	178.03
13	32.64	54.48	68.35	78.37	86.03	92.10	97.11	101.27	104.81
16	7.76	14.57	19.70	23.82	27.24	30.11	32.58	34.74	36.64
19	11.94	7.89	5.36	3.49	2.07	0.93	0.03	0.82	1.49
22	0	0	0	0	0	0	0	0	0

4. Conclusion

⑴Adopting double-ring infiltration apparatus to measure field soil infiltration parameters, inbuilt-ring depth has obvious effect on measuring accuracy. The inbuilt-ring depth ruled by international is smaller and the measured infiltration rate value is bigger than the truth-value.

⑵ Measuring error decreases gradually along with the increase of the inbuilt-ring depth. When the depth reached 19cm～22cm, its relative error could be ignored.

⑶Considering measurement precision, instrument cost and labor intensity, if the buried plough bottom is less than 20cm, the reasonable inbuilt-ring depth should be 19cm; if the buried plough bottom is more than 20cm, the reasonable inbuilt-ring depth should be 20～22cm.

References:

1. Xuezhuan Li, Guisheng Fan.: Influence of organic matter content on infiltration capacity and parameter in field soils [J].Transactions of the CSAE, 22(3):188-190 (2006)
2. Xuezhuan Li, Guisheng Fan.: Experimental study on main factors influencing the infiltration capacity of unsaturated earth canal [J].Journal of hydraulic Engineering, 40(5):630-634, (2009)
3. Jianbin Lai, Yi Luo, Li Ren.: Effects of Buffer-Index of the Double-Ring Infiltrometer on Saturated Hydraulic Conductivity Measurements, Acta Pedologica Sinica, 47(1): 19-25 , (2010)
4. Guisheng Fan, Zhiliang Dang.: Approach on Infiltration Reducing Mechanism of Infiltration under Surge Irrigation [J]. Bulletin of Soil and Water Conservation, 13(6):30-33 (1993)
5. Wenyan Xie, Guisheng Fan.: Influence of moisture content on infiltration characteristics in field soils. [J]. Journal of Taiyuan University of Technology, 35(3): 273-275, (2004)
6. Quanjiu Wang, R Horton, Jun Fan. An analytical solution for one-dimensional water infiltration and redistribution in unsaturated soil, Pedosphere, 19(1)：104-110, (2009)
7. T.S. Moroke, O.Dikinya, C. Patrick.: Comparative assessment of water infiltration of soils under different tillage systems in eastern Botswana. Physics and Chemistry of the Earth, 2009, 34: 316–323 (2009)
8. Jianting, Zhu Binayak, P. Mohanty.: Effective scaling factor for transient infiltration in heterogeneous soils.. Journal of Hydrology, 319: 96–108, (2006)